THE JOURNAL OF PHYSICAL CHEMISTRY C

Article

Cite This: J. Phys. Chem. C 2018, 122, 2297−2306

pubs.acs.org/JPCC

Twisted Donor−Acceptor Cruciform Luminophores Possessing Substituent-Dependent Properties of Aggregation-Induced Emission and Mechanofluorochromism

Yonghui Wang,[†,∥] Defang Xu,[‡,∥] Huaizhi Gao,[†] Ying Wang,[†] Xingliang Liu,*[,†] Aixia Han,[†] Chao Zhang,[†] and Ling Zang*[,§]

[†]Chemical Engineering College, and [‡]State Key Laboratory of Plateau Ecology and Agriculture, Qinghai University, Xining 810016, Qinghai, China

[§]Department of Materials Science and Engineering, University of Utah, Salt Lake City, Utah 84108, United States

Supporting Information

ABSTRACT: Three donor−acceptor (D−A)-containing cruciform luminophores, named **DHCS-BC**, **DMCS-BC**, and **DTCS-BC**, with twisted molecular conformation have been synthesized. The D−A-type cross-conjugated compounds showed unique intramolecular charge transfer (ICT) properties. Interestingly, they showed substituent-dependent aggregation-induced emission (AIE) and mechanofluorochromic (MFC) behavior. The three cruciforms possessed evident AIE nature with the AIE factors of 9, 19, and >492 and high solid-state fluorescence quantum yields of 0.332, 0.425, and 0.492, respectively. Moreover, their AIE activities increased in the order **DHCS-BC** < **DMCS-BC** < **DTCS-BC**, which was consistent with the torsional degree of molecular spatial conformations induced by the steric hindrance between carbazole and substituted cyanostyryl and the ICT degrees of the three compounds. The solid emission studies illustrated that their fluorescence color could change reversibly between bright blue-green (485 nm), bright blue-green (479 nm), bright yellow (526 nm) and light yellow-green (524 nm), yellow-green (534 nm), orange-red (606 nm) through grinding and dichloromethane (DCM) fuming treatment, giving the large spectral red-shifts of 39, 55, and 80 nm, respectively. The MFC activities of the three compounds are increased with the sequence of **DHCS-BC** < **DMCS-BC** < **DTCS-BC**, which was the result of the planarization of the molecular conformation and subsequent planar intramolecular charge transfer (PICT) under the external force stimuli.

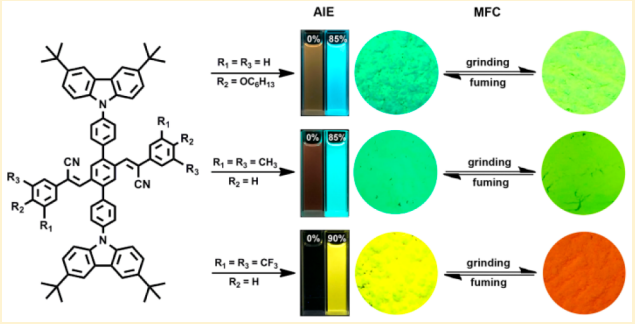

INTRODUCTION

Mechanofluorochromic (MFC) compounds[1−5] that change their solid-state emission color in response to external force stimuli (such as grinding, pressing, shearing, deformation, etc.) have received a great deal of attention from both fundamental research fields of solid-state photochemistry and applications in mechanosensors,[6,7] memory devices,[8,9] fluorescent switches,[10−12] security systems,[13,14] and optoelectronic devices.[15,16] Recently, some MFC molecules based on α-cyano-substituted stilbene,[17−19] tetraphenylethene,[20−25] 9,10-divinylanthracene,[26−34] triphenylacrylonitrile,[35,36] and organoboron complexes[37−44] have been developed. However, MFC materials possessing strong solid-state luminescence and an obvious color contrast are still rare. One of the main reasons is the fact that many π-conjugated luminophores show very weak emission in their aggregated states despite being strongly emissive in dilute solutions. This effect is referred to as the notorious aggregation-caused emission quenching (ACQ).[45,46] To overcome this problem, the aggregation-induced emission (AIE)-active molecules,[47,48] which show strong emission only in the aggregated and solid states, are a promising candidate. Indeed, some MFC materials with strong solid-state emission have been developed based on AIE-active molecules. Since Park's group reported the cyano-distyrylbenzene derivative that exhibits both AIE and MFC behavior in 2010,[17] a number of new AIE MFC compounds have been developed.[27,28] However, even with the use of the AIE strategy, the number of AIE MFC luminophores that exhibit both high solid-state luminescence efficiency and an obvious color contrast remain extremely rare. Therefore, carrying out more extensive explorations to develop novel and general π-systems with both AIE and MFC properties are significant and attractive.

Extended π-conjugated cruciform fluorophores constructed by two π-conjugated arms intersecting at a central aromatic core have attracted considerable attention since their rigid π-conjugated skeletons bring about a set of desired properties and potential applications in chemosensors,[49−53] nonlinear optical materials,[54,55] and organic light-emitting diodes (OLED).[56]

Received: November 17, 2017
Revised: December 23, 2017
Published: January 11, 2018

DOI: 10.1021/acs.jpcc.7b11368
J. Phys. Chem. C 2018, 122, 2297−2306

Chart 1. Molecular Structures of DHCS-BC, DMCS-BC, and DTCS-BC

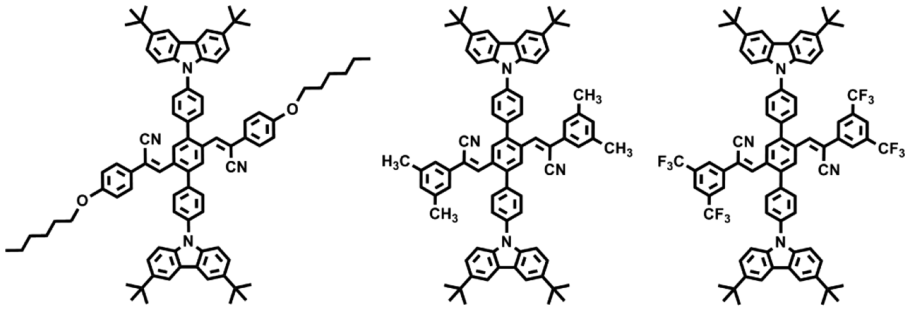

With appropriate donor and acceptor substitution, these compounds localize their frontier molecular orbitals (FMOs) on different portions of the molecule, and thus result in compounds possessing FMOs that are spatially disjoint from one another; in these cases, the highest occupied molecular orbital (HOMO) and lowest unoccupied molecular orbital (LUMO) localize on the crossed arms. This spatial isolation of FMOs makes molecular cruciforms promising candidates for a variety of optoelectronic applications. Herein, we synthesized three new twisted donor−acceptor cruciforms, **DHCS-BC**, **DMCS-BC**, and **DTCS-BC** (Chart 1), and investigated the influence of molecular structures on photophysical properties from the perspective of electronic and steric effects. The three compounds possess the same molecular conjugated backbone. Among them, one of the axes is donor (carbazole) substituted and the other axis is acceptor (cyanostyryl) substituted, and thus species with independent electronic shifts into opposite directions in HOMO and LUMO, i.e., spatially separated FMOs, could be attained. Moreover, the steric hindrance derived from the four bulky substituents attaching on the central benzene endows the three compounds with torsional molecular conformation, resulting in effective depression of close π-packing and enhancement of emission quantum yields in the solid states. Results illustrated that these three compounds exhibit unique intramolecular charge transfer (ICT) nature from one axis to the other in the excited state. Moreover, they showed obvious AIE characteristics and high-contrast MFC behavior with the same order of **DHCS-BC** < **DMCS-BC** < **DTCS-BC**, which depended on electronic and steric effects of the peripheral substituents on the acceptor dicyanodistyrylbenzene axis with two *p*-hexyloxy, four *m*-methyl, to four *m*-trifluoromethyl linkages.

EXPERIMENTAL SECTION

General. ^{1}H and ^{13}C NMR spectra were recorded on a Bruker-Avance III (400 MHz) spectrometer by using $CDCl_3$ as the solvents. UV−vis spectra were obtained on a Shimadzu UV-2550 spectrophotometer. Fluorescence measurements were performed on a Cary Eclipse fluorescence spectrophotometer. The absolute fluorescence quantum yields for **DHCS-BC**, **DMCS-BC**, and **DTCS-BC** were measured on an Edinburgh FLS920 steady-state spectrometer using an integrating sphere. High-resolution mass spectra (HRMS) were recorded on a MALDI-TOF MS Performance (Shimadzu, Japan). Elemental analyses were performed with a PerkinElmer 240C elemental analyzer by investigation of C, H, and N. X-ray diffraction (XRD) patterns were obtained on a Bruker D8 Focus powder X-ray diffraction instrument. The calculations for **DHCS-BC**, **DMCS-BC**, and **DTCS-BC** were based on the density functional theory (DFT) and performed at the B3LYP/6-31G(d) level using the Gaussian 09W program package.

Materials. Tetrahydrofuran (THF) was distilled from sodium and benzophenone under nitrogen immediately prior to use. Ethanol was distilled under normal pressure over sodium under nitrogen before use. The other chemicals were used as received without further purification. Compound **2** was synthesized according to the literature.[57]

Preparation of the Samples for Aggregation-Induced Emission Study. The water/THF mixtures with different water fractions were prepared by slowly adding distilled water into solutions of the target molecules in THF under sonication at room temperature, the concentration was maintained at 1.0×10^{-5} M. The fluorescence emission spectral measurement of the mixture was performed immediately.

Preparation of the Samples for Mechanofluorochromism Study. The ground powders were prepared by grinding the as-prepared powders with a pestle in the mortar. The fumed samples were obtained by fuming the ground powder with dichloromethane (DCM) for 2 min.

Synthesis. *4,4′′-Bis(3,6-di-tert-butyl-9H-carbazol-9-yl)-[1,1′:4′,1′′-terphenyl]-2′,5′-dicarbaldehyde (**3**).* Compounds **1** (4.50 g, 15.42 mmol) and **2** (20.00 g, 41.54 mmol), $Pd(PPh_3)_4$ (150 mg, 0.130 mmol), Na_2CO_3 (9.00 g, 84.91 mmol), and tetrabutylammonium hydrogen sulfate (1.50 g, 4.42 mmol) were added into toluene/H_2O (450 mL, v/v = 3/2). The mixture was heated to reflux under nitrogen atmosphere for 24 h. After cooling to room temperature, the organic layer was separated, the aqueous layer was extracted with CH_2Cl_2 (2 × 100 mL), and the combined organic layer was dried over anhydrous Na_2SO_4. Upon evaporating off the solvent, the crude product was subjected to purification by column chromatography by (silica gel, CH_2Cl_2/petroleum ether, v/v = 2/1), affording a yellow solid (8.15 g). Yield 63%. ^{1}H NMR (400 MHz, $CDCl_3$) δ: 10.33 (s, 2H), 8.31 (s, 2H), 8.20 (s, 4H), 7.80 (d, J = 8.4 Hz, 4H), 7.72 (d, J = 8.0 Hz, 4H), 7.56−7.49 (m, 8H), 1.51 (s, 36H) (Figures S19 and S20, Supporting Information). ^{13}C NMR (100 MHz, $CDCl_3$) δ: 191.49, 143.90, 143.40, 139.04, 138.91, 136.69, 134.65, 131.48, 130.58, 126.70, 123.82, 123.72, 116.41, 109.19, 34.79, 32.02 (Figure S21, Supporting Information). HRMS (MALDI-TOF) m/z: $[M]^+$ calcd for $C_{60}H_{60}N_2O_2$, 840.4655; found, 840.4668 (Figure S22, Supporting Information). Anal. Calcd (%) for $C_{60}H_{60}N_2O_2$: C, 85.68; H, 7.19; N, 3.33. Found: C, 85.61; H, 7.26; N, 3.29.

(2Z,2′Z)-3,3′-(4,4′′-Bis(3,6-di-tert-butyl-9H-carbazol-9-yl)-[1,1′:4′,1′′-terphenyl]-2′,5′-diyl)bis(2-(4-(hexyloxy)phenyl)-

DOI: 10.1021/acs.jpcc.7b11368
J. Phys. Chem. C 2018, 122, 2297−2306

Scheme 1. Synthetic Routes of DHCS-BC, DMCS-BC, and DTCS-BC

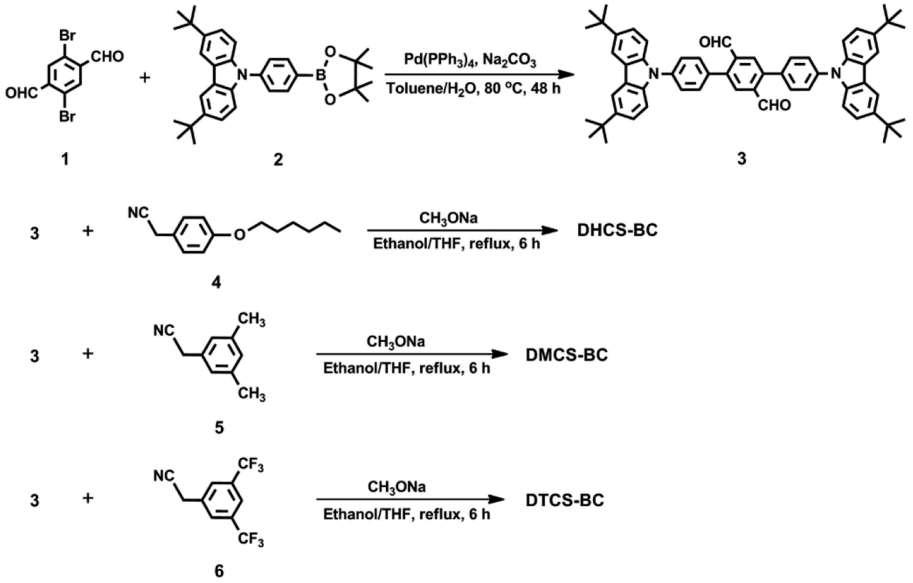

*acrylonitrile) (**DHCS-BC**).* Compounds **3** (1.50 g, 1.78 mmol) and **4** (1.16 g, 5.35 mmol) were added into dry ethanol (50 mL) and dry THF (5 mL), and then CH_3ONa (0.29 g, 5.35 mmol) was added quickly. The mixture was refluxed with stirring for 24 h under an atmosphere of nitrogen. After cooling to room temperature, the resulting precipitate was collected by filtration and dried under vacuum. The crude product was purified by column chromatography (silica gel, CH_2Cl_2), affording a light yellow-green solid (1.62 g). Yield 73%. ^{1}H NMR (400 MHz, $CDCl_3$) δ: 8.43 (d, J = 9.2 Hz, 2H), 8.20 (d, J = 8.8 Hz, 4H), 7.80−7.74 (m, 8H), 7.60 (t, J = 4.4 Hz, J = 4.4 Hz, 6H), 7.54−7.48 (m, 8H), 6.98 (d, J = 9.2 Hz, 4H), 4.03 (t, J = 6.4 Hz, J = 6.8 Hz, 4H), 1.86−1.78 (m, 4H), 1.51 (s, 36H), 1.48−1.44 (m, 4H), 1.39−7.35 (m, 8H), 0.93 (t, J = 7.2 Hz, J = 6.8 Hz, 6H) (Figures S23 and S24, Supporting Information). ^{13}C NMR (100 MHz, $CDCl_3$) δ: 160.42, 143.24, 140.77, 139.07, 138.50, 138.44, 137.42, 133.76, 131.46, 130.52, 127.45, 126.49, 126.23, 123.70, 118.08, 116.30, 115.22, 114.07, 109.31, 68.33, 34.74, 31.99, 31.50, 29.11, 25.63, 22.51, 13.90 (Figure S25, Supporting Information). HRMS (MALDI-TOF) m/z: $[M]^+$ calcd for $C_{88}H_{94}N_4O_2$, 1238.7377; found, 1238.7389 (Figure S26, Supporting Information). Anal. Calcd (%) for $C_{88}H_{94}N_4O_2$: C, 85.26; H, 7.64; N, 4.52. Found: C, 85.19; H, 7.70; N, 4.60.

*(2Z,2′Z)-3,3′-(4,4′′-Bis(3,6-di-tert-butyl-9H-carbazol-9-yl)-[1,1′:4′,1′′-terphenyl]-2′,5′-diyl)bis(2-(3,5-dimethylphenyl)-acrylonitrile) (**DMCS-BC**).* By following the synthetic procedure for **DHCS-BC**, **DMCS-BC** was synthesized by using **3** (1.60 g, 1.90 mmol), **5** (0.69 g, 4.75 mmol), and CH_3ONa (0.26 g, 4.81 mmol) as the reagents. The crude product was purified by column chromatography (silica gel, CH_2Cl_2/petroleum ether, v/v = 3/1), affording a light yellow solid (1.48 g). Yield 71%. ^{1}H NMR (400 MHz, $CDCl_3$) δ: 8.44 (s, 2H), 8.19 (s, 4H), 7.82−7.74 (m, 10H), 7.52 (s, 8H), 7.32 (s, 4H), 7.09 (s, 2H), 2.42 (s, 12H), 1.51 (s, 36H) (Figures S27 and S28, Supporting Information). ^{13}C NMR (100 MHz, $CDCl_3$) δ: 143.23, 140.77, 140.60, 138.98, 138.93, 138.45, 137.20, 133.76, 131.54, 131.39, 130.71, 126.51, 124.01, 123.70, 123.65, 118.19, 116.35, 114.70, 109.27, 34.76, 32.01, 21.38 (Figure S29, Supporting Information). HRMS (MALDI-TOF) m/z: $[M]^+$ calcd for $C_{80}H_{78}N_4$, 1094.6226; found, 1094.6239 (Figure S30, Supporting Information). Anal. Calcd (%) for $C_{80}H_{78}N_4$: C, 87.71; H, 7.18; N, 5.11. Found: C, 87.78; H, 7.27; N, 5.06.

*(2Z,2′Z)-3,3′-(4,4′′-Bis(3,6-di-tert-butyl-9H-carbazol-9-yl)-[1,1′:4′,1′′-terphenyl]-2′,5′-diyl)bis(2-(3,5-bis-(trifluoromethyl)phenyl)acrylonitrile) (**DTCS-BC**).* By following the synthetic procedure for **DHCS-BC**, **DTCS-BC** was synthesized by using **3** (1.60 g, 1.90 mmol), **6** (1.20 g, 4.74 mmol), and CH_3ONa (0.26 g, 4.81 mmol) as the reagents. The crude product was purified by column chromatography (silica gel, CH_2Cl_2), affording a yellow-green solid (1.79 g). Yield 72%. ^{1}H NMR (400 MHz, $CDCl_3$) δ: 8.52 (s, 2H), 8.18 (s, 4H), 8.13 (s, 4H), 7.98 (s, 2H), 7.92 (s, 2H), 7.82−7.77 (m, 8H), 7.53−7.45 (m, 8H), 1.51 (s, 36H) (Figures S31 and S32, Supporting Information). HRMS (MALDI-TOF) m/z: $[M]^+$ calcd for $C_{80}H_{66}F_{12}N_4$, 1310.5096; found, 1310.5084 (Figure S33, Supporting Information). Anal. Calcd (%) for $C_{80}H_{66}F_{12}N_4$: C, 73.27; H, 5.07; N, 4.27. Found: C, 73.35; H, 5.16; N, 4.35.

RESULTS AND DISCUSSION

Synthesis of DHCS-BC, DMCS-BC, and DTCS-BC. The synthetic routes for three compounds **DHCS-BC**, **DMCS-BC**, and **DTCS-BC** are shown in Scheme 1. The precursor **3** was prepared by Suzuki−Miyaura coupling reaction between **1** and **2** catalyzed by $Pd(PPh_3)_4$ in toluene/H_2O in a yield of 63%, and then **3** was allowed to react with **4**−**6** via standard Knoevenagel condensation in the presence of sodium methoxide, respectively, to give the target molecules **DHCS-BC**, **DMCS-BC**, and **DTCS-BC** with good yields of above 70%. All the intermediates and target molecules were characterized by ^{1}H and ^{13}C NMR, matrix-assisted laser desorption ionization time-of-flight (MALDI-TOF) mass spectrometry, and C, H, N elemental analyses. **DHCS-BC**, **DMCS-BC**, and **DTCS-BC** are soluble in common organic solvents, such as $CHCl_3$, CH_2Cl_2, THF, benzene, and toluene, but show poor solubility in alcohols and aliphatic hydrocarbon solvents, such as cyclohexane, *n*-hexane, methanol, and ethanol.

UV−Vis Absorption and Fluorescence Emission Spectra in Solutions. The solvent effect on the absorption

DOI: 10.1021/acs.jpcc.7b11368
J. Phys. Chem. C 2018, 122, 2297−2306

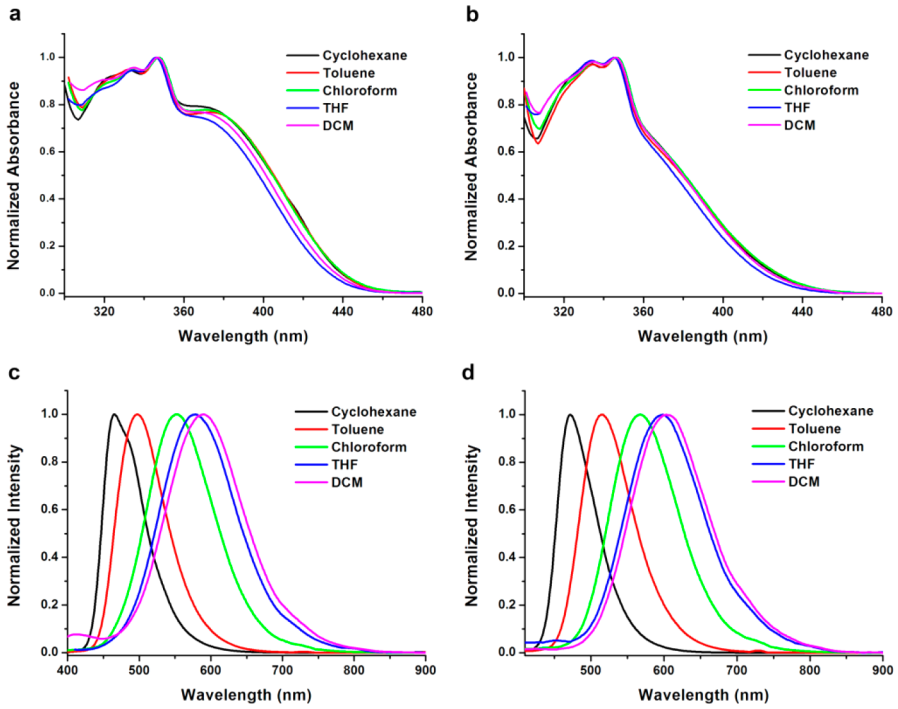

Figure 1. Normalized UV−vis absorption spectra of **DHCS-BC** (a) and **DMCS-BC** (b), and normalized PL spectra of **DHCS-BC** (c) and **DMCS-BC** (d) excited at 365 nm in different solvents (1.0×10^{-5} mol L^{-1}).

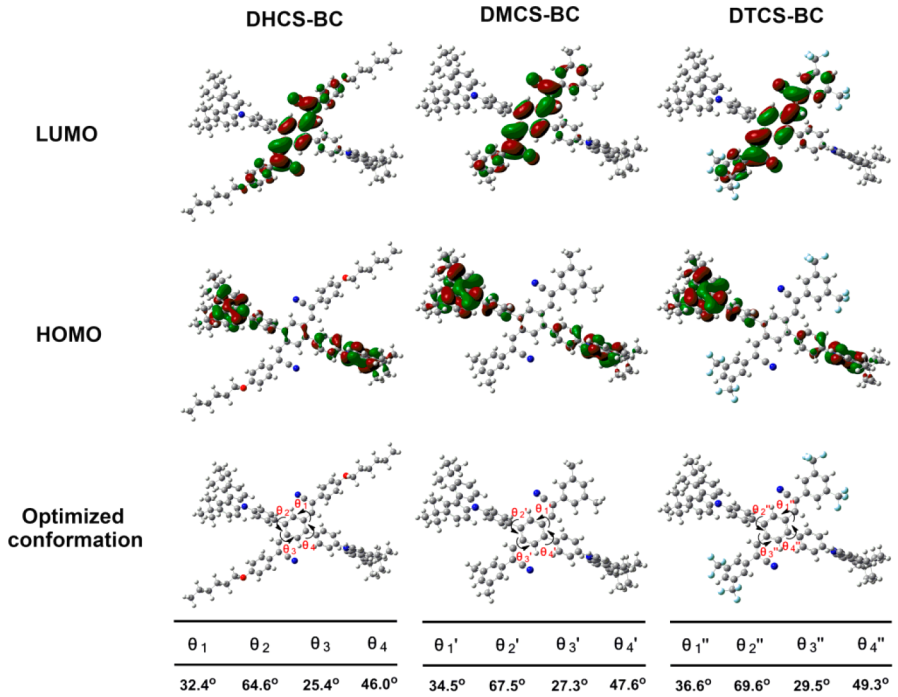

Figure 2. Electron density distributions in the HOMO and LUMO states and optimized conformation of **DHCS-BC**, **DMCS-BC**, and **DTCS-BC** calculated by DFT in Gaussian 09 at the B3LYP/6-31G(d) level.

and fluorescence properties of **DHCS-BC**, **DMCS-BC**, and **DTCS-BC** was examined in various solvents (Figure 1 and Figure S1, Supporting Information), and the corresponding photophysical data are collected in Tables S1−S3 (Supporting Information). It is clear that the three compounds all exhibit three absorption bands. The absorption bands at about 335 and 347 nm might be attributed to the $\pi-\pi^*$ transition, and the weak ones at around 365, 370, and 430 nm correspond to charge-transfer (CT) transition between electron donor (carbaole unit) and electron acceptor (dicyanodistyrylbenzene moiety) (Figure 1, parts a and b, and Figure S1a, Supporting Information).[52] In order to confirm the occurrence of CT transition, the solvent-dependent fluorescence emission spectra of **DHCS-BC**, **DMCS-BC**, and **DTCS-BC** are shown in the Figure 1, parts c and d, and Figure S1b (Supporting Information). It was found that the maximum emission bands

DOI: 10.1021/acs.jpcc.7b11368
J. Phys. Chem. C 2018, 122, 2297−2306

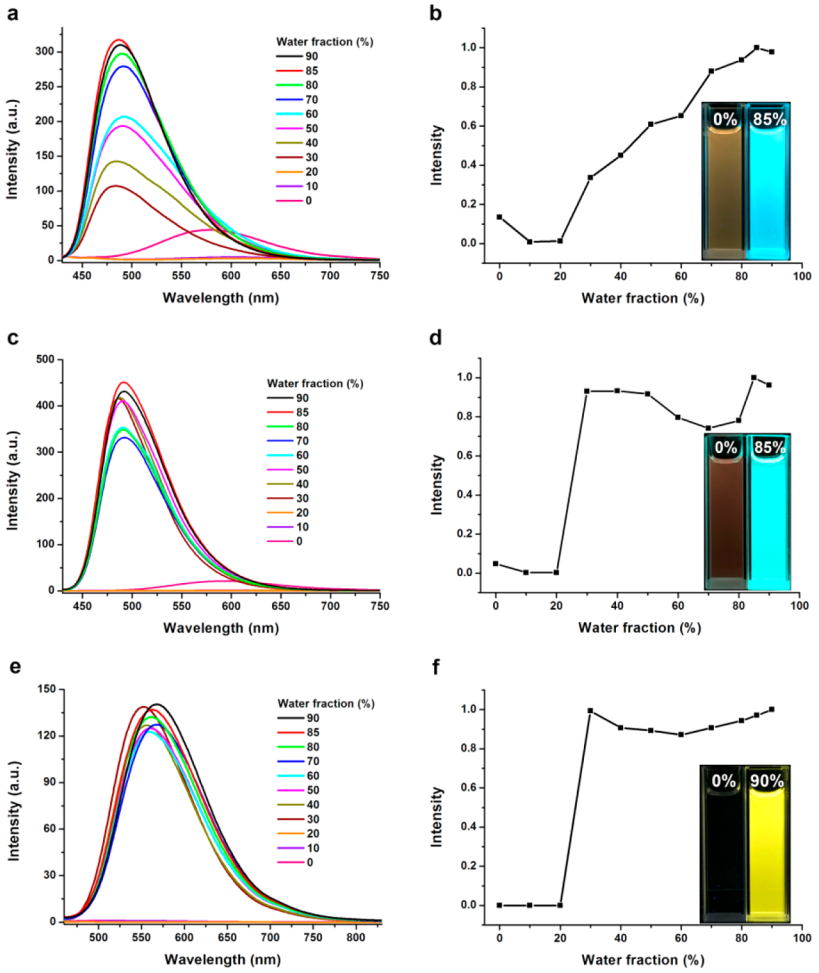

Figure 3. PL spectra of **DHCS-BC** (a), **DMCS-BC** (c), and **DTCS-BC** (e) in THF/water mixtures with different water fractions (λ_{ex} = 400 nm). Normalized fluorescence emission intensities of **DHCS-BC** (b), **DMCS-BC** (d), and **DTCS-BC** (f) in THF/water with different f_w. The inset graphs in panels b, d, and f are the solutions of **DHCS-BC** (f_w = 0% and 85%), **DMCS-BC** (f_w = 0% and 85%), and **DTCS-BC** (f_w = 0% and 90%) in THF/water mixture under UV illumination, respectively.

of the three luminophores became broad and red-shifted significantly with increasing polarity of the solvent. For example, in cyclohexane, **DHCS-BC** exhibited a strong emission band at 465 nm, but with the increasing solvent polarity, its emission band red-shifted to 590 nm in DCM accompanied by emission band broadening. At the same time, the large Stokes shifts of **DHCS-BC** increased from 7396 cm^{-1} in cyclohexane to 11 869 cm^{-1} in DCM (Table S1, Supporting Information). Combined with the large Stokes shifts and the broadening and red-shift of the emission bands, we suggest that intramolecular charge transfer (ICT) transitions of **DHCS-BC** take place in polar solvents[58,59] and the longer wavelength emissions might be assigned to ICT emissions. In addition, the maximum ICT emission wavelengths of the three compounds showed a rising trend in the same solvent, indicating the ICT degrees of them in the excited state increased in the order **DHCS-BC** ≈ **DMCS-BC** < **DTCS-BC**,[52,60] which are the same as the order of the onset wavelength in absorption (Figures S2−S6, Supporting Information). The fluorescence quantum yields (Φ_f) of **DHCS-BC**, **DMCS-BC**, and **DTCS-BC** in different solvents were measured using quinine sulfate (Φ_f = 0.546, 0.5 mol L^{-1} H_2SO_4) as the standard (Tables S1−S3, Supporting Information). It was found that Φ_f of the three compounds decreased significantly with increasing polarity of the solvent, indicating a positive solvatokinetic effect.[43,61] For example, the Φ_f of **DMCS-BC** decrease from 0.278 in cyclohexane to 0.045 in chloroform, and then to 0.020 in dichloromethane. The lower Φ_f value in solution might be ascribed to the active intramolecular rotations of multiple phenyl rings and the strong ICT interaction, which often caused nonirradiative decay. In addition, the Φ_f values are significantly affected by the substituents attached on the periphery of dicyanodistyrylbenzene. For instance, in THF solutions, the Φ_f values are in the order **DHCS-BC** ≈ **DMCS-BC** < **DTCS-BC**, which can be ascribed to the electron-donating or electron-withdrawing ability of the substituents to the conjugated backbone from two *p*-hexyloxy, four *m*-methyl, to four *m*-trifluoromethyl linkages (electronic effect). This is consistent with their ICT degrees of the three compounds in the excited state.

To provide a more effective understanding the influence of the geometric and electronic structures of **DHCS-BC**, **DMCS-BC**, and **DTCS-BC** on their photophysical properties, we employed the theoretical calculation using the DFT method at the B3LYP/6-31G(d) level after optimizing their structures to the lowest energy spatial conformation with the Gaussian 09W program. The frontier orbital plots of the HOMOs and LUMOs are shown in Figure 2. It is clear that the electron

DOI: 10.1021/acs.jpcc.7b11368
J. Phys. Chem. C 2018, 122, 2297−2306

densities in the HOMOs of these three cruciforms are mainly distributed over the donor carbazole units and the central phenyl, whereas the electron densities in the LOMOs are localized along the acceptor dicyanodistyrylbenzene axis. The separated HOMOs and LUMOs further illustrated the occurrence of the effective excited-state ICT process from the donor (carbazole) to the acceptor (dicyanodistyrylbenzene) axis upon excitation, which was in accordance with the results of spectral studies. Moreover, the three molecules adopted a twisted spatial conformation at their optimized lowest energy states. For **DHCS-BC**, the dihedral angles between two vinyl planes and the central benzene are 32.4° and 25.4°, respectively, and the dihedral angles between two side benzene rings and the central core are 64.6° and 46.0°, respectively. For **DMCS-BC** and **DTCS-BC**, the corresponding dihedral angles increased to 34.5°, 27.3°, 67.5°, 47.6° and 36.6°, 29.5°, 69.6°, 49.3°, respectively. Obviously, such high torsional angles in the three molecules should be ascribed to the steric hindrance between carbazole and substituted cyanostyryl groups. The distortion degree of molecular conformation of these three compounds increased with the sequence of **DHCS-BC** < **DMCS-BC** < **DTCS-BC**, which is consistent with steric hindrance between carbazole and cyanostyryl induced by the substituents to the conjugated backbone from *p*-hexyloxy, *m*-methyl, to *m*-trifluoromethyl linkages. The specially twisted conformation would inhibit close packing and $\pi-\pi$ interactions in the condensed state, leading to strong solid-state emission, AIE characteristics, and MFC behavior.

Aggregation-Induced Emission. When illuminated under a UV lamp, both **DHCS-BC** and **DMCS-BC** could emit strong blue-green light and **DTCS-BC** could give bright yellow light in the powder states, but weak fluorescence was observed from their dilute THF solutions. Therefore, we speculate that they would possess AIE properties. To confirm the AIE nature of **DHCS-BC**, **DMCS-BC**, and **DTCS-BC**, we measured their photoluminescence (PL) spectra in dilute mixtures of water/THF with different water fractions (f_w, the volume percentage of water in THF/water mixtures). Water is used because it is a nonsolvent for the compounds and increasing the water fraction in the mixed solvents can change its existing form from a solution state in THF to aggregated particles in mixtures with certain water content. As shown in Figure 3, parts a, c, and e, the three compounds displayed similar fluorescent behavior. In dilute THF solutions, **DHCS-BC** and **DMCS-BC** could emit orange and wine-red fluorescence and the maxima peaks appears at 581 and 598 nm, respectively, but the intensity was weak and Φ_f were only 0.036 and 0.022. For **DTCS-BC**, its PL intensity was so weak that almost no signal could be detected from its dilute THF solution, and its Φ_f was below 0.001. In the region where f_w was less than 20%, the PL intensities of the three compounds showed a gradually declining trend and the emission peak wavelengths exhibited a gradual bathochromic shift. These observations could be explained by the solvatochromic effect. **DHCS-BC**, **DMCS-BC**, and **DTCS-BC** are typical donor−acceptor (D−A) molecular structure; the ICT between the D and A moieties in molecules is enhanced with the increase of the environment polarity, which is offered by increasing the water fraction. Afterward, the PL intensities started to increase rapidly at the f_w of 20% for the three compounds, at which solvating powers of the mixtures were worsened to such an extent that the luminogen molecules began to aggregate. As the f_w value in the THF solution increased to 85% for **DHCS-BC** and **DMCS-BC** and 90% for **DTCS-BC**, the emission intensities of the three cruciforms were approximately 7-, 5-, and 160-fold higher than those in pure THF and a strong blue (486 nm), blue-green (493 nm), and yellow (568 nm) emission could be observed, respectively, thus proving their AIE nature (Figure 3, parts b, d, and f). The weak emissive nature of the luminogens in THF and aqueous mixtures with low f_w values (<20%) should be ascribed to the active intramolecular rotations and the strong ICT process of the genuinely dissolved luminogens, which effectively consume the energy of the excitons nonradiatively. However, an increase in the f_w value of the mixed solvent led to the transformation of the luminogens from the dissolved and well-dispersed state in pure THF to aggregated particles in THF/water mixtures (f_w > 20%), resulting in restricted internal rotations (RIR) accompanied by limited ICT effect, which prevented the nonradiative relaxation channels and thus made the aqueous mixture highly emissive. To further confirm the aggregate formation, dynamic light scattering (DLS) technique was used to characterize the obtained aggregated particles and revealed the existence of nanoaggregates as their main constituent (Figures S7−S9, Supporting Information). The fluorescence images showed the emission of the compounds in the solvent mixtures at f_w = 0% and 90% under 365 nm UV light at room temperature (insets of parts b, d, and f of Figure 3). It was clear that **DHCS-BC**, **DMCS-BC**, and **DTCS-BC** in THF solutions showed very weak fluorescence, but very strong fluorescence was observed in THF/water mixtures with high water content, thus further indicating that the compounds had a strong AIE effect.

To quantitatively evaluate the AIE effect of **DHCS-BC**, **DMCS-BC**, and **DTCS-BC**, the fluorescence quantum yields of the luminogens in solution ($\Phi_{f,s}$) and as-prepared solid ($\Phi_{f,aps}$) states were determined. The $\Phi_{f,aps}$ values for **DHCS-BC**, **DMCS-BC**, and **DTCS-BC** are 0.332, 0.425, and 0.492, respectively, which are considerably boosted compared to those in pure THF (0.036, 0.022, and <0.001), giving AIE factors ($\alpha_{AIE} = \Phi_{f,aps}/\Phi_{f,s}$) of 9, 19, and >492 with respect to those in THF. In addition, as can be seen from the above results, the AIE activities of these three compounds increased in the order **DHCS-BC** < **DMCS-BC** < **DTCS-BC**, which is consistent with the distortion degree of molecular conformation of these three compounds.

Mechanofluorochromic Properties. In our previous study, we found that, for the π-conjugated luminogens with the twisted architectures, the AIE feature and ICT characteristics usually exhibited tuned emissions in response to mechanical stimuli.[33−35] Herein, **DHCS-BC**, **DMCS-BC**, and **DTCS-BC** were greatly anticipated to be MFC-active materials. To check whether the three luminogens exhibited mechanochromic luminescence, their solid emission properties were studied. As shown in Figure 4, parts b, d, and f, the as-prepared **DHCS-BC**, **DMCS-BC**, and **DTCS-BC** solids could emit bright blue-green, bright blue-green, and bright yellow light under UV irradiation (Figures S10−S12, Supporting Information), and their emitting colors changed into light yellow-green, yellow-green, and orange-red light, respectively, after grinding by using a spatula or a pestle, indicating the obvious MFC behavior of the three luminogens. PL spectra were used to monitored the above naked-eye-visible fluorescence color changes, and the emission bands of samples obtained under different conditions (grinding and fuming) are illustrated in Figure 4, parts a, c, and e. The emission peaks of the three compounds in the as-prepared powders appear at 485, 479, and

DOI: 10.1021/acs.jpcc.7b11368
J. Phys. Chem. C 2018, 122, 2297−2306

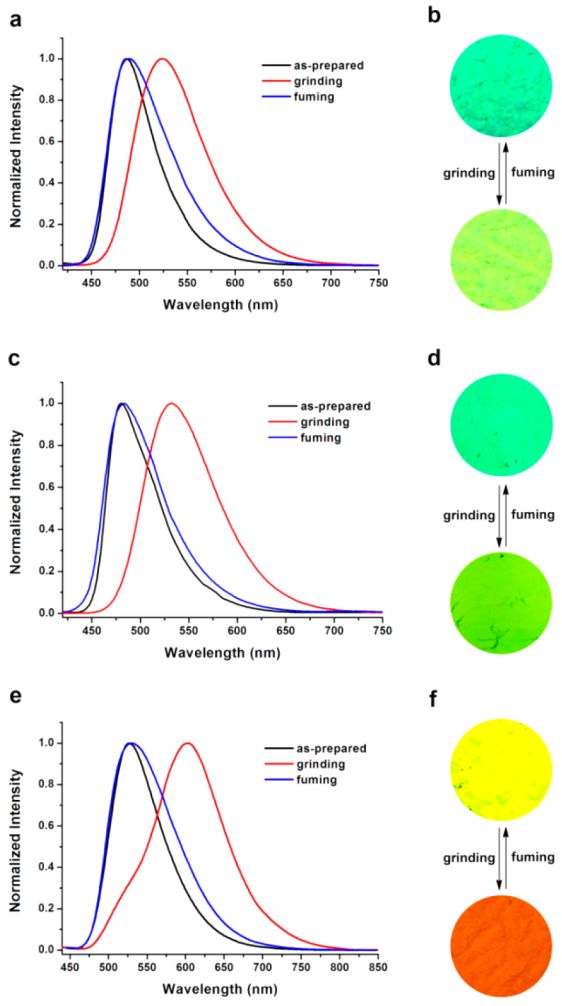

Figure 4. Normalized fluorescence spectra of **DHCS-BC** (a), **DMCS-BC** (c), and **DTCS-BC** (e) excited at 365 nm in different solid states: as-prepared, grinding, and fuming. Photographs of **DHCS-BC** (b), **DMCS-BC** (d), and **DTCS-BC** (f) color changes under grinding and fuming stimuli.

526 nm and red-shift to 524, 534, and 606 nm in the ground powders, respectively, indicating that the grinding treatment induced the spectral shifts of 39, 55, and 80 nm for three luminogens. Moreover, after fuming with the vapor of DCM for several seconds at room temperature, the fluorescence colors were recovered to the original ones, similar to their as-prepared powders, and the corresponding maximum emission wavelengths could blue-shift to the initial ones. When the fumed samples were reground, the fluorescence colors changed as the first grinding again. The wavelength changes in solid-state emission could be repeated many times without fatigue, suggesting excellent reversibility in the switching processes (Figures S13–S15, Supporting Information).

To understand the origin of the MFC behavior of **DHCS-BC**, **DMCS-BC**, and **DTCS-BC**, the XRD measurements were performed on the respective samples, and the diffraction patterns are shown in Figure 5a–c. Clearly, the XRD patterns of the as-prepared samples solids show many intense and sharp diffraction peaks, suggesting a well-ordered microcrystalline-like structure (Figures S10–S12, Supporting Information). By sharp contrast, after the as-prepared solids of the three compounds were ground, the XRD patterns showed significant decreased peak intensity but increased peak widths, suggesting that the

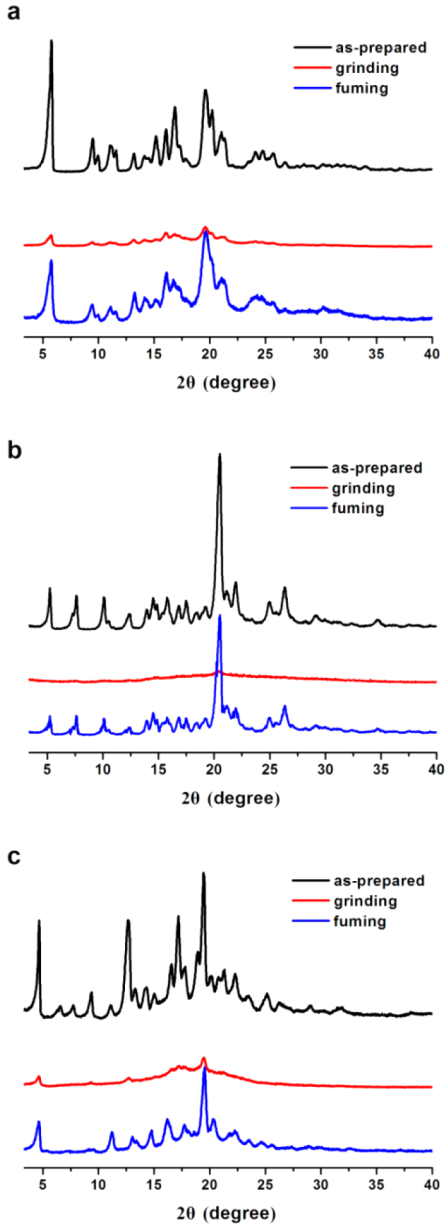

Figure 5. XRD patterns of **DHCS-BC** (a), **DMCS-BC** (b), and **DTCS-BC** (c) in different solid states: as-prepared, grinding, and fuming.

crystalline state was damaged into amorphous state during the grinding process (mechanical force). When the ground powders were fumed with DCM, sharp and strong diffraction peaks, similar to those of the crystals, appeared again, meaning that the molecules in the amorphous state could be rearranged into an ordered crystalline state. The XRD results strongly suggested that the reversible mechanochromism of **DHCS-BC**, **DMCS-BC**, and **DTCS-BC** was directly caused by the phase transformation between the ordered crystalline and the disordered amorphous states. The absorption spectrum of the three compounds in cyclohexane solutions displayed absorption bands with vibronic structures, and their absorption maximum appear at 346, 346, and 348 nm, respectively. Then, in the solid states the absorption bands red-shift to 432, 437, and 442 nm, thus indicating the existence of significant π–stack and J-aggregates that were formed in the solid states. Generally, the destruction of the crystalline structure leads to the planarization

DOI: 10.1021/acs.jpcc.7b11368
J. Phys. Chem. C 2018, 122, 2297–2306

of the molecular conformation due to the release of the twist strain. This phenomenon is one of the possible reasons for the increase in molecular conjugation resulting in a red-shift in the PL spectrum. However, in this case, the large red-shifts of the luminogens after grinding might be original from the conformational change and rotate to a position more parallel to the coplanar under external pressure, leading to extended conjugation and subsequent planar intramolecular charge transfer (PICT). This proposal could be evidenced by the UV−vis absorption spectra of as-prepared and ground samples (Figures S16−S18, Supporting Information). It was clear that the ground **DHCS-BC**, **DMCS-BC**, and **DTCS-BC** samples showed the obvious red-shifts of the onset wavelengths relative to that of as-prepared samples, indicating the extension of π-conjugation after grinding.[24] For **DTCS-BC**, it displayed the maximum spectral red-shift due to its most twisted molecular conformation and largest CT degrees in the excited state in the three luminogens. In the case of **DHCS-BC** and **DMCS-BC**, although they exhibited the similar CT degrees in the excited state, **DMCS-BC** possessed more twisted molecular conformation than **DHCS-BC**, which was an advantage to the red-shift of the PL spectrum under external force. Therefore, the MFC activities of the three compounds are increased in a sequence of **DHCS-BC** < **DMCS-BC** < **DTCS-BC**, and the planarization of the molecular conformation and subsequent PICT account for the MFC behavior of such torsional cruciforms.

CONCLUSIONS

Three twisted D−A-substituted benzene-centered cruciforms, **DHCS-BC**, **DMCS-BC**, and **DTCS-BC**, have been designed and successfully synthesized. The three cross-conjugated compounds possess spatially separated HOMOs and LUMOs located on the donor and acceptor axes, respectively. Such D−A-type cruciforms show unique ICT emission from the donor (carbazole) to the acceptor (dicyanodistyrylbenzene) axis upon excitation. More importantly, the three compounds show substituent-dependent AIE characteristics and MFC behavior. The AIE and MFC activities of these three compounds increased with the same order of **DHCS-BC** < **DMCS-BC** < **DTCS-BC**; the former are influenced by the torsional degrees of molecular spatial conformations induced by the steric hindrance of the substituents linked on cyanostyryl moieties, and the latter are ascribed to the planarization of the molecular conformation and subsequent PICT with mechanical stimuli. The general structure−property relationship established here will provide a possible strategy for designing new AIE MFC dyes that have potential application in optical-recording and pressure-sensing materials.

ASSOCIATED CONTENT

Supporting Information

The Supporting Information is available free of charge on the ACS Publications website at DOI: 10.1021/acs.jpcc.7b11368.

Photophysical data, UV−vis spectra and PL spectra in dilute solutions, DLS data, fluorescence microscope images, reversibility of MFC processes, UV−vis absorption spectra of as-prepared and ground samples, and NMR spectra and HRMS of **3**, **DHCS-BC**, **DMCS-BC**, and **DTCS-BC** (PDF)

AUTHOR INFORMATION

Corresponding Authors

*E-mail: liuxl1219@163.com.

*E-mail: lzang@eng.utah.edu.

ORCID

Xingliang Liu: 0000-0003-2883-5766

Author Contributions

‖Yonghui Wang and Defang Xu contributed equally.

Notes

The authors declare no competing financial interest.

ACKNOWLEDGMENTS

This work was financially supported by the National Natural Science Foundation of China (NNSFC, nos. 21362027 and 21662028), Qinghai Province "High-end Innovative Thousand Talents Plan" (2017), and the China Scholarship Council (CSC).

REFERENCES

(1) Caruso, M. M.; Davis, D. A.; Shen, Q.; Odom, S. A.; Sottos, N. R.; White, S. R.; Moore, J. S. Mechanically-induced chemical changes in polymeric materials. *Chem. Rev.* **2009**, *109*, 5755−5798.

(2) Chi, Z.; Zhang, X.; Xu, B.; Zhou, X.; Ma, C.; Zhang, Y.; Liu, S.; Xu, J. Recent advances in organic mechanofluorochromic materials. *Chem. Soc. Rev.* **2012**, *41*, 3878−3896.

(3) Xue, P.; Ding, J.; Wang, P.; Lu, R. Recent progress in the mechanochromism of phosphorescent organic molecules and metal complexes. *J. Mater. Chem. C* **2016**, *4*, 6688−6706.

(4) Zhang, X.; Chi, Z.; Zhang, Y.; Liu, S.; Xu, J. Recent advances in mechanochromic luminescent metal complexes. *J. Mater. Chem. C* **2013**, *1*, 3376−3390.

(5) Xue, S.; Qiu, X.; Sun, Q.; Yang, W. Alkyl length effects on solid-state fluorescence and mechanochromic behavior of small organic luminophores. *J. Mater. Chem. C* **2016**, *4*, 1568−1578.

(6) Kinami, M.; Crenshaw, B. R.; Weder, C. Polyesters with built-in threshold temperature and deformation sensors. *Chem. Mater.* **2006**, *18*, 946−955.

(7) Park, D.-H.; Hong, J.; Park, I. S.; Lee, C. W.; Kim, J.-M. A Colorimetric hydrocarbon sensor employing a swelling-induced mechanochromic polydiacetylene. *Adv. Funct. Mater.* **2014**, *24*, 5186−5193.

(8) Irie, M.; Fukaminato, T.; Sasaki, T.; Tamai, N.; Kawai, T. Organic chemistry: A digital fluorescent molecular photoswitch. *Nature* **2002**, *420*, 759−760.

(9) Lim, S. J.; An, B. K.; Jung, S. D.; Chung, M. A.; Park, S. Y. Photoswitchable organic nanoparticles and a polymer film employing multifunctional molecules with enhanced fluorescence emission and bistable photochromism. *Angew. Chem., Int. Ed.* **2004**, *43*, 6346−6350.

(10) Ma, Z.; Teng, M.; Wang, Z.; Yang, S.; Jia, X. Mechanically induced multicolor switching based on a single organic molecule. *Angew. Chem., Int. Ed.* **2013**, *52*, 12268−12272.

(11) Kwon, M. S.; Gierschner, J.; Seo, J.; Park, S. Y. Rationally designed molecular D−A−D triad for piezochromic and acidochromic fluorescence on−off switching. *J. Mater. Chem. C* **2014**, *2*, 2552−2557.

(12) Cheng, X.; Li, D.; Zhang, Z.; Zhang, H.; Wang, Y. Organoboron compounds with morphology-dependent NIR emissions and dual-channel fluorescent ON/OFF switching. *Org. Lett.* **2014**, *16*, 880−883.

(13) Kishimura, A.; Yamashita, T.; Yamaguchi, K.; Aida, T. Rewritable phosphorescent paper by the control of competing kinetic and thermodynamic self-assembling events. *Nat. Mater.* **2005**, *4*, 546−549.

(14) Zhu, X.; Liu, R.; Li, Y.; Huang, H.; Wang, Q.; Wang, D.; Zhu, X.; Liu, S.; Zhu, H. An AIE-active boron-difluoride complex: multi-stimuli-responsive fluorescence and application in data security protection. *Chem. Commun.* **2014**, *50*, 12951−12954.

(15) Yuan, W. Z.; Gong, Y. G.; Chen, S. M.; Shen, X. Y.; Lam, J. W. Y.; Lu, P.; Lu, Y. W.; Wang, Z. M.; Hu, R. R.; Xie, N.; et al. Efficient solid emitters with aggregation-induced emission and intramolecular charge transfer characteristics: molecular design, synthesis, photophysical behaviors, and OLED application. *Chem. Mater.* **2012**, *24*, 1518−1528.
(16) Gong, Y. Y.; Zhang, Y. R.; Yuan, W. Z.; Sun, J. Z.; Zhang, Y. M. D−A solid emitter with crowded and remarkably twisted conformations exhibiting multifunctionality and multicolor mechanochromism. *J. Phys. Chem. C* **2014**, *118*, 10998−11005.
(17) Yoon, S.-J.; Chung, J. W.; Gierschner, J.; Kim, K. S.; Choi, M.-G.; Kim, D.; Park, S. Y. Multistimuli two-color luminescence switching via different slip-stacking of highly fluorescent molecular sheets. *J. Am. Chem. Soc.* **2010**, *132*, 13675−13683.
(18) Yoon, S.-J.; Park, S. Y. J. Polymorphic and mechanochromic luminescence modulation in the highly emissive dicyanodistyrylbenzene crystal: secondary bonding interaction in molecular stacking assembly. *J. Mater. Chem.* **2011**, *21*, 8338−8346.
(19) Kunzelman, J.; Kinami, M.; Crenshaw, B. R.; Protasiewicz, J. D.; Weder, C. Oligo(*p*-phenylene vinylene)s as a "new" class of piezochromic fluorophores. *Adv. Mater.* **2008**, *20*, 119−122.
(20) Shen, X. Y.; Wang, Y. J.; Zhao, E.; Yuan, W. Z.; Liu, Y.; Lu, P.; Qin, A.; Ma, Y.; Sun, J. Z.; Tang, B. Z. Effects of substitution with donor−acceptor groups on the properties of tetraphenylethene trimer: aggregation-induced emission, solvatochromism, and mechanochromism. *J. Phys. Chem. C* **2013**, *117*, 7334−7347.
(21) Luo, X.; Zhao, W.; Shi, J.; Li, C.; Liu, Z.; Bo, Z.; Dong, Y.; Tang, B. Z. Reversible switching emissions of tetraphenylethene derivatives among multiple colors with solvent vapor, mechanical, and thermal stimuli. *J. Phys. Chem. C* **2012**, *116*, 21967−21972.
(22) Misra, R.; Jadhav, T.; Dhokale, B.; Mobin, S. M. Reversible mechanochromism and enhanced AIE in tetraphenylethene substituted phenanthroimidazoles. *Chem. Commun.* **2014**, *50*, 9076−9078.
(23) Lu, Q.; Li, X.; Li, J.; Yang, Z.; Xu, B.; Chi, Z.; Xu, J.; Zhang, Y. Influence of cyano groups on the properties of piezofluorochromic aggregation-induced emission enhancement compounds derived from tetraphenylvinyl-capped ethane. *J. Mater. Chem. C* **2015**, *3*, 1225−1234.
(24) Zhang, X.; Chi, Z.; Xu, B.; Chen, C.; Zhou, X.; Zhang, Y.; Liu, S.; Xu, J. End-group effects of piezofluorochromic aggregation-induced enhanced emission compounds containing distyrylanthracene. *J. Mater. Chem.* **2012**, *22*, 18505−18513.
(25) Peng, Z.; Huang, K.; Tao, Y.; Li, X.; Zhang, L.; Lu, P.; Wang, Y. Turning on the solid emission from non-emissive 2-aryl-3-cyanobenzofurans by tethering tetraphenylethene for green electroluminescence. *Mater. Chem. Front.* **2017**, *1*, 1858−1865.
(26) Dong, Y.; Xu, B.; Zhang, J.; Tan, X.; Wang, L.; Chen, J.; Lv, H.; Wen, S.; Li, B.; Ye, L.; et al. Piezochromic luminescence based on the molecular aggregation of 9,10-bis((*E*)-2-(pyrid-2-yl)vinyl)anthracene. *Angew. Chem., Int. Ed.* **2012**, *51*, 10782−10785.
(27) Zhang, X.; Chi, Z.; Xu, B.; Jiang, L.; Zhou, X.; Zhang, Y.; Liu, S.; Xu, J. Multifunctional organic fluorescent materials derived from 9,10-distyrylanthracene with alkoxyl endgroups of various lengths. *Chem. Commun.* **2012**, *48*, 10895−10897.
(28) Zhang, X.; Chi, Z.; Zhang, J.; Li, H.; Xu, B.; Li, X.; Liu, S.; Zhang, Y.; Xu, J. Piezofluorochromic properties and mechanism of an aggregation-induced emission enhancement compound containing *N*-hexyl-phenothiazine and anthracene moieties. *J. Phys. Chem. B* **2011**, *115*, 7606−7611.
(29) Sagara, Y.; Yamane, S.; Mutai, T.; Araki, K.; Kato, T. A stimuli-responsive, photoluminescent, anthracene-based liquid crystal: emission color determined by thermal and mechanical processes. *Adv. Funct. Mater.* **2009**, *19*, 1869−1875.
(30) Liu, W.; Wang, Y.; Sun, M.; Zhang, D.; Zheng, M.; Yang, W. Alkoxy-position effects on piezofluorochromism and aggregation-induced emission of 9,10-bis(alkoxystyryl)anthracenes. *Chem. Commun.* **2013**, *49*, 6042−6044.
(31) Xue, S.; Liu, W.; Qiu, X.; Gao, Y.; Yang, W. Remarkable isomeric effects on optical and optoelectronic properties of *N*-phenylcarbazole-capped 9,10-divinylanthracenes. *J. Phys. Chem. C* **2014**, *118*, 18668−18675.
(32) Zheng, M.; Zhang, D.; Sun, M.; Li, Y.; Liu, T.; Xue, S.; Yang, W. Cruciform 9,10-distyryl-2,6-bis(*p*-dialkylamino-styryl)anthracene homologues exhibiting alkyl length-tunable piezochromic luminescence and heat-recovery temperature of ground states. *J. Mater. Chem. C* **2014**, *2*, 1913−1920.
(33) Bu, L.; Sun, M.; Zhang, D.; Liu, W.; Wang, Y.; Zheng, M.; Xue, S.; Yang, W. Solid-state fluorescence properties and reversible piezochromic luminescence of aggregation-induced emission-active 9,10-bis[(9,9-dialkylfluorene-2-yl)vinyl]anthracenes. *J. Mater. Chem. C* **2013**, *1*, 2028−2035.
(34) Wang, Y.; Liu, W.; Bu, L.; Li, J.; Zheng, M.; Zhang, D.; Sun, M.; Tao, Y.; Xue, S.; Yang, W. Reversible piezochromic luminescence of 9,10-bis[(*N*-alkylcarbazol-3-yl)vinyl]anthracenes and the dependence on *N*-alkyl chain length. *J. Mater. Chem. C* **2013**, *1*, 856−862.
(35) Gong, Y.; Tan, Y.; Liu, J.; Lu, P.; Feng, C.; Yuan, W. Z.; Lu, Y.; Sun, J. Z.; He, G.; Zhang, Y. Twisted D−π−A solid emitters: efficient emission and high contrast mechanochromism. *Chem. Commun.* **2013**, *49*, 4009−4011.
(36) Yuan, W. Z.; Tan, Y.; Gong, Y.; Lu, P.; Lam, J. W. Y.; Shen, X. Y.; Feng, C.; Sung, H. H.-Y.; Lu, Y.; Williams, I. D.; et al. Synergy between twisted conformation and effective intermolecular interactions: strategy for efficient mechanochromic luminogens with high contrast. *Adv. Mater.* **2013**, *25*, 2837−2843.
(37) Zhang, G.; Lu, J.; Sabat, M.; Fraser, C. L. Polymorphism and reversible mechanochromic luminescence for solid-state difluoroboron avobenzone. *J. Am. Chem. Soc.* **2010**, *132*, 2160−2162.
(38) Zhou, L.; Xu, D.; Gao, H.; Han, A.; Liu, X.; Zhang, C.; Li, Z.; Yang, Y. Triphenylamine functionalized β-Ketoiminate boron complex exhibiting aggregation-induced emission and mechanofluorochromism. *Dyes Pigm.* **2017**, *137*, 200−207.
(39) Gao, H.; Xu, D.; Liu, X.; Han, A.; Zhou, L.; Zhang, C.; Li, Z.; Dang, J. Tetraphenylethene-based β-diketonate boron complex: efficient aggregation-induced emission and high contrast mechanofluorochromism. *Dyes Pigm.* **2017**, *139*, 157−165.
(40) Zhou, L.; Xu, D.; Gao, H.; Han, A.; Yang, Y.; Zhang, C.; Liu, X.; Zhao, F. Effects of cyano groups on the properties of thiazole-based β-ketoiminate boron complexes: aggregation-induced emission and mechanofluorochromism. *RSC Adv.* **2016**, *6*, 69560−69568.
(41) Galer, P.; Korošec, R. C.; Vidmar, M.; Šket, B. Crystal structures and emission properties of the BF_2 complex 1-phenyl-3-(3,5-dimethoxyphenyl)-propane-1,3-dione: multiple chromisms, aggregation- or crystallization-induced emission, and the self-assembly effect. *J. Am. Chem. Soc.* **2014**, *136*, 7383−7394.
(42) Wang, X.; Liu, Q.; Yan, H.; Liu, Z.; Yao, M.; Zhang, Q.; Gong, S.; He, W. Piezochromic luminescence behaviors of two new benzothiazole−enamido boron difluoride complexes: intra- and inter-molecular effects induced by hydrostatic compression. *Chem. Commun.* **2015**, *51*, 7497−7500.
(43) Zhang, Z.; Xue, P.; Gong, P.; Zhang, G.; Peng, J.; Lu, R. Mechanofluorochromic behaviors of β-iminoenolate boron complexes functionalized with carbazole. *J. Mater. Chem. C* **2014**, *2*, 9543−9551.
(44) Yoshii, R.; Suenaga, K.; Tanaka, K.; Chujo, Y. Mechanofluorochromic materials based on aggregation-induced emission-active boron ketoiminates: regulation of the direction of the emission color changes. *Chem. - Eur. J.* **2015**, *21*, 7231−7237.
(45) Liu, J.; Lam, J. W. Y.; Tang, B. Z. Acetylenic solymers: syntheses, structures, and functions. *Chem. Rev.* **2009**, *109*, 5799−5867.
(46) Hong, Y. N.; Lam, J. W. Y.; Tang, B. Z. Aggregation-induced emission. *Chem. Soc. Rev.* **2011**, *40*, 5361−5388.
(47) Luo, J.; Xie, Z.; Lam, J. W. Y.; Cheng, L.; Chen, H.; Qiu, C.; Kwok, H. S.; Zhan, X.; Liu, Y.; Zhu, D.; et al. Aggregation-induced emission of 1-methyl-1,2,3,4,5-pentaphenylsilole. *Chem. Commun.* **2001**, *0*, 1740−1741.
(48) Mei, J.; Leung, N. L. C.; Kwok, R. T. K.; Lam, J. W. Y.; Tang, B. Z. Aggregation-induced emission: together we shine, united we soar! *Chem. Rev.* **2015**, *115*, 11718−11940.

DOI: 10.1021/acs.jpcc.7b11368
J. Phys. Chem. C 2018, 122, 2297−2306

(49) Saeed, M. A.; Le, H. T. M.; Miljanic, O. S. Benzobisoxazole cruciforms as fluorescent sensors. *Acc. Chem. Res.* **2014**, *47*, 2074−2083.
(50) Wilson, J. N.; Bunz, U. H. F. Switching of intramolecular charge transfer in cruciforms: metal ion sensing. *J. Am. Chem. Soc.* **2005**, *127*, 4124−4125.
(51) Sun, J.; Lv, X.; Wang, P.; Zhang, Y.; Dai, Y.; Wu, Q.; Ouyang, M.; Zhang, C. A donor−acceptor cruciform π-system: high contrast mechanochromic properties and multicolour electrochromic behavior. *J. Mater. Chem. C* **2014**, *2*, 5365−5371.
(52) Sun, J.; Dai, Y.; Ouyang, M.; Zhang, Y.; Zhan, L.; Zhang, C. Unique torsional cruciform π-architectures composed of donor and acceptor axes exhibiting mechanochromic and electrochromic properties. *J. Mater. Chem. C* **2015**, *3*, 3356−3363.
(53) Liu, W.; Wang, J.; Gao, Y.; Sun, Q.; Xue, S.; Yang, W. 2,6,9,10-Tetra(*p*-dibutylaminostyryl)anthracene as a multifunctional fluorescent cruciform dye. *J. Mater. Chem. C* **2014**, *2*, 9028−9034.
(54) He, F.; Tian, L.; Tian, X.; Xu, H.; Wang, Y.; Xie, W.; Hanif, M.; Xia, J.; Shen, F.; Yang, B.; Li, F.; Ma, Y. G.; Yang, Y. Q.; Shen, J. C. Diphenylamine-substituted cruciform oligo(phenylene vinylene): enhanced one- and two-photon excited fluorescence in the solid state. *Adv. Funct. Mater.* **2007**, *17*, 1551−1557.
(55) Dalton, G. T.; Cifuentes, M. P.; Petrie, S.; Stranger, R.; Humphrey, M. G.; Samoc, M. Independent switching of cubic nonlinear optical properties in a ruthenium alkynyl cruciform complex by employing protic and electrochemical stimuli. *J. Am. Chem. Soc.* **2007**, *129*, 11882−11883.
(56) Xie, Z.; Yang, B.; Li, F.; Cheng, G.; Liu, L.; Yang, G.; Xu, H.; Ye, L.; Hanif, M.; Liu, S.; et al. Cross dipole stacking in the crystal of distyrylbenzene derivative: the approach toward high solid-state luminescence efficiency. *J. Am. Chem. Soc.* **2005**, *127*, 14152−14153.
(57) Yu, M.; Wang, S.; Shao, S.; Ding, J.; Wang, L.; Jing, X.; Wang, F. Starburst 4,4′,4″-tris(carbazol-9-yl)-triphenylamine-based deep-blue fluorescent emitters with tunable oligophenyl length for solution-processed undoped organic light-emitting diodes. *J. Mater. Chem. C* **2015**, *3*, 861−869.
(58) Yang, J.-S.; Liau, K.-L.; Wang, C.-M.; Hwang, C.-Y. Substituent-dependent photoinduced intramolecular charge transfer in *N*-aryl-substituted *trans*-4-aminostilbenes. *J. Am. Chem. Soc.* **2004**, *126*, 12325−12335.
(59) Liu, X.; Xu, D.; Lu, R.; Li, B.; Qian, C.; Xue, P.; Zhang, X.; Zhou, H. Luminescent organic 1D nanomaterials based on bis(β-diketone)carbazole derivatives. *Chem. - Eur. J.* **2011**, *17*, 1660−1669.
(60) Sun, W.; Zhou, C.; Xu, C.-H.; Zhang, Y.-Q.; Li, Z.-X.; Fang, C.-J.; Sun, L.-D.; Yan, C.-H. Intramolecular charge transfer in 5-methoxy-2-(2-pyridyl)thiazole-derived fluorescent molecules with different acceptor or donor substituents. *J. Phys. Chem. A* **2009**, *113*, 8635−8646.
(61) Wu, S. K. The problem on photophysics and photochemistry of organic compounds possessing ability of fluorescence emission. *Prog. Chem.* **2005**, *17*, 15−39.

DOI: 10.1021/acs.jpcc.7b11368
J. Phys. Chem. C 2018, 122, 2297−2306